

## On the propagation and decay of North Brazil Current rings

Kerstin Jochumsen,<sup>1,2</sup> Monika Rhein,<sup>1</sup> Sabine Hüttl-Kabus,<sup>1,3</sup> and Claus W. Böning<sup>4</sup>

Received 7 December 2009; revised 25 June 2010; accepted 29 June 2010; published 2 October 2010.

[1] Near the western boundary of the tropical North Atlantic, where the North Brazil Current (NBC) retroflects into the North Equatorial Countercurrent, large anticyclonic rings are shed. After separating from the retroflexion region, the so-called NBC rings travel northwestward along the Brazilian coast, until they reach the island chain of the Lesser Antilles and disintegrate. These rings contribute substantially to the upper limb return flow of the Atlantic Meridional Overturning Circulation by carrying South Atlantic Water into the northern subtropical gyre. Their relevance for the northward transport of South Atlantic Water depends on the frequency of their generation as well as on their horizontal and vertical structure. The ring shedding and propagation and the complex interaction of the rings with the Lesser Antilles are investigated in the  $\frac{1}{12}^\circ$  Family of Linked Atlantic Model Experiments (FLAME) model. The ring properties simulated in FLAME reach the upper limit of the observed rings in diameter and agree with recent observations on seasonal variability, which indicates a maximum shedding during the first half of the year. When the rings reach the shallow topography of the Lesser Antilles, they are trapped by the island triangle of St. Lucia, Barbados and Tobago and interact with the island chain. The model provides a resolution that is capable of resolving the complex topographic conditions at the islands and illuminates various possible fates for the water contained in the rings. It also reproduces laboratory experiments that indicate that both cyclones and anticyclones are formed after a ring passes through a topographic gap. Trajectories of artificial floats, which were inserted into the modeled velocity field, are used to investigate the pathways of the ring cores and their fate after they encounter the Lesser Antilles. The majority of the floats entered the Caribbean, while the northward Atlantic pathway was found to be of minor importance. No prominent pathway was found east of Barbados, where a ring could avoid the interaction with the islands and migrate toward the northern Lesser Antilles undisturbed.

**Citation:** Jochumsen, K., M. Rhein, S. Hüttl-Kabus, and C. W. Böning (2010), On the propagation and decay of North Brazil Current rings, *J. Geophys. Res.*, 115, C10004, doi:10.1029/2009JC006042.

### 1. Introduction

[2] The connection between the equatorial Atlantic and the Caribbean Sea, and the transport pathways of South Atlantic Water (SAW) into the Northern Hemisphere, have been topics of research for some time [e.g., Halliwell *et al.*, 2003; Garzoli *et al.*, 2004]. A major contribution to the cross-hemispheric exchange is provided by large anticyclonic eddies, which propagate northward along the South American coast [Ffield, 2005]. The eddy-shedding occurs at the retroflexion of the North Brazil Current (NBC), which crosses the

equator at the western boundary and turns eastward near  $7^\circ\text{N}$  into the North Equatorial Countercurrent (NECC). The retroflexion is schematically depicted in Figure 1. The resulting eddies, so-called NBC rings, migrate northwestward and reach the Lesser Antilles virtually undisturbed, with nearly pure SAW in their cores [e.g., Fratantoni and Glickson, 2002]. The transport of SAW within the NBC rings represents an important mechanism for the northward flow of the Atlantic Meridional Overturning Circulation (AMOC) and thus is of considerable importance for understanding the meridional heat transports in the Atlantic.

[3] One of the first long-term current meter records of the NBC retroflexion and the ring shedding was collected by Johns *et al.* [1990], who moored instruments near French Guiana. The authors noticed a 50 day oscillation in the current records throughout the year, which they associated with the shedding of NBC rings, although the NBC retroflexion was found to follow a seasonal cycle. Since that time various studies on the NBC retroflexion, the ring shedding and its importance for the interhemispheric exchange have been carried out (some examples are Ffield [2005], Stramma *et al.*

<sup>1</sup>Institut für Umweltphysik, Abteilung Ozeanographie, Universität Bremen, Bremen, Germany.

<sup>2</sup>Now at Institut für Meereskunde, Universität Hamburg, Hamburg, Germany.

<sup>3</sup>Now at Bundesamt für Seeschifffahrt und Hydrographie, Hamburg, Germany.

<sup>4</sup>Leibniz Institut für Meereswissenschaften, Universität Kiel, Kiel, Germany.

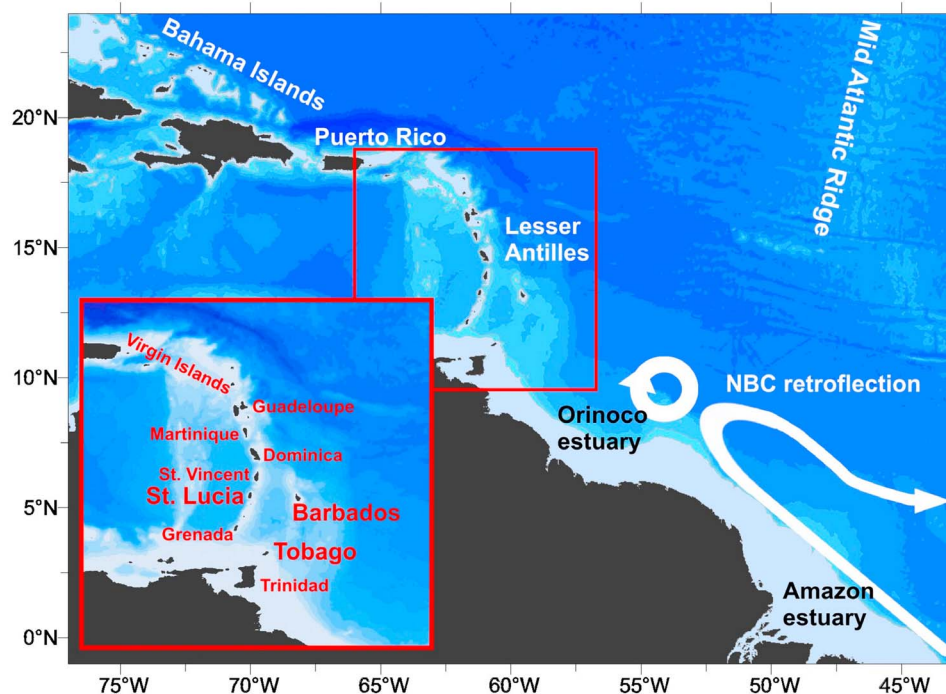


**Figure 1.** Topography of the western tropical North Atlantic with the North Brazil Current (NBC) and its retroreflection indicated in white, as well as an exemplary NBC ring north of the retroreflection. The complicated topography of the Lesser Antilles island arc is shown in detail in the inset.

[2005], and Halliwell *et al.* [2003]). Time series of detailed observations, e.g., the analysis of altimeter data by Goni and Johns [2003], confirmed the continuous ring shedding and reported a weak tendency to enhanced ring production during the first half of the year. In contrast a pronounced seasonal cycle was identified in the strength of the NBC retroreflection, where the maximum transport develops from July to December (with a peak in September) and the minimum passes in March and April [Garzoli *et al.*, 2004]. As a cause for the ring shedding different mechanisms were investigated, e.g., Jochum and Malanotte-Rizzoli [2003] found the reflection of baroclinic Rossby waves at the coast to create NBC rings. Recently, Zharkov and Nof [2009] presented results from a theoretical approach and numerical simulations of the NBC, which showed that the coastal slant of South America is a crucial factor for the ring generation. The averaged inclination of the entire coastline near the NBC retroreflection induces the constant ring shedding in their model, despite the seasonal cycle of the NBC retroreflection, and they form a relatively stable chain, propagating along the coast.

[4] The vertical structure may differ dramatically between single NBC rings [Wilson *et al.*, 2002], therefore three different types of rings are distinguished: shallow and surface intensified rings, deep reaching and surface intensified rings and deep reaching and subsurface intensified rings. The rings affect the layer thickness of the water masses contained in a ring by thickening the density layers where the ring core is located. Surface intensified rings involve an accumulation of Tropical Surface Waters in their center; they are associated with a positive sea surface height anomaly, clearly marking

the rings in satellite altimetry data [cf. Goni and Johns, 2003]. For subsurface rings, the effect on the sea level is rather small, since only a thickening of the upper thermocline occurs, therefore they cannot be traced at the sea surface and are missing in studies using satellite data only.

[5] Concerning the propagation, fate and decay of the rings, many questions are still unanswered. While their generation and movement toward the Caribbean has been observed several times, the understanding of subsurface types and the ring demise is incomplete. The complicated topography of the Lesser Antilles island arc (Figure 1), which separates the Atlantic Ocean from the Caribbean Sea, prohibits the undisturbed northwestward propagation of NBC rings. Some rings presumably get trapped at the topography of the Lesser Antilles, but some might remain in the Atlantic and continue their northward migration east of the island arc. Fratantoni and Richardson [2006] analyzed the structure, evolution and partly demise of 10 NBC rings near the Lesser Antilles by surface drifter and subsurface float data. They suggested a separation of rings at 200–300 m, in an upper and a lower part, at the latitude of Tobago. The shallow part was found to propagate further northwestward, while the deeper part remained near Tobago, interacting with subsequent rings. Ring-ring interactions were found to be commonplace in their study.

[6] Rhein *et al.* [2005] reported both surface and subsurface intensified NBC rings at the latitude of Guadeloupe (at 16°N), off the continental shelf. No permanent northward flow was found at the western boundary current, the transport was instead achieved by NBC rings. Using temperature and salinity data the rings were easily identified by

their high SAW signatures, as well as repeating changes of current direction in the velocity field, obtained from the current profiler observations. During their ship surveys the structure of the rings encountered varied in shape and distinctiveness, but on every of the five cruises at least one ring could be identified. Therefore a permanent pathway is expected to exist, which allows the rings to propagate nearly undisturbed to 16°N.

[7] The transport into the Caribbean Sea through the various passages of the Lesser Antilles was analyzed by *Kirchner et al.* [2008]. The authors laid their focus especially on the South Atlantic Water fraction of the inflow, which represents an important part of the AMOC. The work was based on a comparison of data from observations with the high-resolution ocean model FLAME, where the model was found to capture the salient features of the inflow through the various small passages. The model and the observations showed high consistency in the strength of the mean total inflow, its range of variability and the general distribution of SAW. The observed water masses were simulated accurately as well. In a subsequent study that simulation was used to analyze the spreading of southern water masses within and northward of the equatorial gyre, complementing findings from Argo data [*Kirchner et al.*, 2009].

[8] *Mertens et al.* [2009] combined moored instruments in the triangle between Tobago, Barbados and St. Lucia with altimeter data to study the role of NBC rings for the transport variability of the Caribbean inflow. During the mooring time period (June 2003 to September 2005), 13 SSH anomalies were found and attributed to rings, and 10 of them reached the mooring array. In general the advent of a ring coincided with high baroclinic velocity variability in the moored array. One additional event was found without corresponding SSH signal, which was attributed to a deep ring without surface expression.

[9] In this study we extend the analysis of the FLAME simulation to investigate the NBC ring shedding period and its variability for all three ring types near the NBC retro-reflection, as well as the propagation of the rings and their decay. The main questions addressed in this work are as follows: (1) Can a high-resolution ocean model reproduce the vertical structure and behavior of NBC rings? (2) How strong is the impact of subsurface types and how many rings reach into depths below the thermocline? (3) What is the result of the interaction of NBC rings with the topography of the Lesser Antilles? Is an undisturbed pathway to 16°N realized in the model? (4) Do the subsurface intensified rings reveal different propagation pathways to the surface intensified types? (5) What is the contribution of the rings to the cross hemispheric volume transport?

## 2. Model and Methods

### 2.1. The FLAME Model

[10] Used in this study is a high-resolution ( $\frac{1}{12}^\circ$ ) version of the ocean model FLAME (Family of Linked Atlantic Model Experiments [*Dengg et al.*, 1999]), applied to the Atlantic Ocean between 70°N and 18°S [e.g., *Eden and Böning*, 2002]. The model is based on the Modular Ocean Model code [MOM2.1; *Pacanowski*, 1995] and solves the primitive equations on an isotropic Arakawa B grid [*Arakawa*,

1966] in a  $z$  coordinate system. The simulation considered here uses a horizontal grid of  $\frac{1}{12}^\circ$  and 45 vertical levels, with a 10 m resolution at the surface, smoothly increasing to a maximum of 250 m below 2250 m. The temperature and salinity fields of inflowing water at the open northern and southern boundaries are damped toward climatological values; the barotropic flow at the northern boundary is taken from the Arctic model of *Brauch and Gerdes* [2005], while at the southern boundary, it is calculated from stream function values (obtained by the Sverdrup relation).

[11] Vertical mixing is parameterized on the basis of a stability-dependent approach for vertical diffusivity and viscosity, as described in the work of *Böning and Kröger* [2005], and the wind-induced mixing in the surface layers is calculated following *Kraus and Turner* [1967]. More detailed information on the model configuration is given in the work of *Hüttl-Kabus and Böning* [2008].

[12] The bathymetry in FLAME lacks some detail in the area of complex topography, such as the Lesser Antilles passages (e.g., missing some of the deep parts, see *Kirchner et al.* [2008] for details). The Lesser Antilles are represented as shallow ocean points and are still about 35 m deep. When investigating NBC rings near this topographic barrier, the focus is therefore on the deeper layers below 35 m, where a more realistic interaction with the island topography can be expected. In coastal areas the effects of river runoffs, e.g., the Amazon and Congo, were implicitly accounted for in the relaxation of salinity to low-salinity caps near the river mouths.

[13] The spin-up of the model started from a climatology based on a combination of *Levitus and Boyer* [1994] and *Boyer and Levitus* [1997]; the following 15 year run included interannual variability and is used in this study. This variable surface forcing is build on a climatological ECMWF mean [*Barnier et al.*, 1995] and supplemented by interannual anomalies of the NCEP/NCAR reanalyses [*Kalnay et al.*, 1996].

[14] The model has been used previously for several studies in the Tropical Atlantic, e.g., in the works of *Hüttl and Böning* [2006] and *Kirchner et al.* [2009]; a variant of the model was also used by *Brandt and Eden* [2005]. The study of *Kirchner et al.* [2008] included a detailed model data comparison, indicating a realistic model behavior with respect to observed mean transports and its variability. Thus, earlier studies validated the model and showed that FLAME is suitable for applications in the tropical North Atlantic.

[15] A previous study by *Garraffo et al.* [2003] already used a high-resolution model to analyze aspects of the ring shedding and their propagation. In contrast to the FLAME model, their simulation based on MICOM (Miami Isopycnic Coordinate Ocean Model) lacked high-frequency and inter-annual variability in the forcing, since only monthly climatological data sets were used (COADS [see *da Silva et al.*, 1994]). While their results reflected climatological conditions, the FLAME simulation considered here extends the investigation of the NBC rings to behaviors in their varying environment.

[16] *Garraffo et al.* [2003] focused their study on the ring shedding, the classification of the different types, their sea surface height signature and methods of transport estimates. In our study we extend the analysis of the ring shedding in FLAME to the fate and decay of the rings near the Lesser

Antilles and provide an analysis of artificial floats to track the core waters of the NBC rings.

## 2.2. Identification of South Atlantic Water

[17] Previous studies based on observations have shown that NBC rings contain a distinct core of South Atlantic Water (SAW), which differs in temperature and salinity from the surrounding water [e.g., *Johns et al.*, 2003, *Rhein et al.*, 2005]. The exact percentage of SAW can be obtained by a water mass analysis, which identifies the SAW by its distinct temperature and salinity signature. Similar to applications with hydrographic ocean measurements, the water mass analysis can be applied on the model data as well. The method is explained in detail in the work of *Kirchner et al.* [2008], where it was already used on FLAME data near the Lesser Antilles. The analysis calculates the fraction of each source component (which were taken from the Northern/Southern Hemisphere) necessary to obtain the properties of the given water sample. The result is the SAW fraction in percent.

[18] The amount of SAW found in the water of the tropical North Atlantic is dependent on the depth level considered [*Kirchner et al.*, 2009]. The water column of the upper ocean in the research area consists of different layers to the depth of 1100 m, which are distinguished by their characteristic features. This work follows the description by *Stramma and Schott* [1999] and applied by *Rhein et al.* [2005], *Kirchner et al.* [2008], *Mertens et al.* [2009], and *Kirchner et al.* [2009] in the eastern Caribbean and western North Atlantic. In this work the Central Water layer is used for tracking the NBC rings, which occupies the density range of  $\sigma_\theta = 26.3\text{--}27.1 \text{ kg m}^{-3}$  (approximately 200–500 m). This layer is further subdivided into upper and lower Central Water (UCW and LCW; divided at  $\sigma_\theta = 26.8$ ). The thermocline layer known as the Salinity Maximum Water (SMW) is discussed as well ( $\sigma_\theta = 24.5\text{--}26.3 \text{ kg m}^{-3}$ ). The water masses have sources in both hemispheres and a mixture of these sources forms the water in the western tropical North Atlantic. More details can be found in the works of *Rhein et al.* [2005] and *Kirchner et al.* [2009].

## 3. NBC Ring Properties in FLAME

### 3.1. Ring Types and Shedding Rates

[19] Anticyclonic rings are produced in the model at the NBC retroflection, which alters its position periodically in the region between 8°N and 4°N at the South American coast. The rings emerge directly at the retroflection and propagate along the western boundary toward the island arc of the Lesser Antilles. NBC rings can easily be identified in the velocity field, some examples are shown in Figure 2. Depicted are snapshots of the modeled current speed for distinct depth levels. During each time one NBC ring is centered at 54°W, but the spatial and vertical structure is different in those vortices, as illustrated in Figure 3. The NBC rings and the NBC retroflection dominate the instantaneous current field at all times, only within the Caribbean Sea occasionally other strong eddy structures are present.

[20] In October 2002 (Figure 2a) the current speed at 91 m shows the NBC retroflection south of 7°N and two NBC rings further north. A smaller ring is squeezed between the islands of Tobago and Barbados and a Caribbean Eddy

is apparent at 69°W. The NBC ring centered at 54°W is of the shallow, surface intensified type and spans a diameter of 350 km. The vertical structure in Figure 3a shows a distinct velocity maximum near the surface and no deep penetration; the ring is confined to the upper 200 m. The maximum core velocity is 171 cm/s in the zonal direction.

[21] The current speed in January 1999 (Figure 2b) shows a similar ring centered at 54°W, north of the NBC retroflection, which is visible as well at the 91 m depth level. No other significant features are evident in this current field. The vertical structure in Figure 3b reveals a distinct vortex, which is intensified at the surface but extends to 1000 m depth. The maximum velocity in the ring core is 161 cm/s (zonal direction), comparable to the shallow ring of the October 2002 current field, as well as a diameter of 380 km.

[22] In Figure 2c the current speed in October 1999 is depicted at 218 m depth. No other prominent features are evident in the current field. The ring at 54°W has a diameter of 240 km, which is somewhat smaller than the rings found at shallower depth. The vertical structure reveals a subsurface ring core, located between 100 and 350 m (Figure 3c), as well as the ring extension to 950 m depth. The maximum zonal velocity is 85 cm/s, thus weaker than in the surface intensified types.

[23] For the full model period from 1990 to 2004 all rings passing the 54°W section were registered and classified as either surface intensified (shallow or deep reaching) or subsurface intensified types by their imprints in the current speed and SAW content. A time series for the year 2002 is shown in Figure 4. Depicted is the model layer in 91 m depth, where seven NBC rings crossed the section during the whole year. The rings are well structured vortices, with current speeds exceeding 90 cm/s in the swirling area and low-velocity centers. The rings are not only clearly visible in the current speed, but in the SAW content as well. Pronounced high SAW contents occur as distinct events, at times where NBC rings are found in the current speed. The snapshot in October 2002, which was used in Figure 2a, is marked by the red vertical line. The ring was the sixth ring passing the 54°W section in 2002.

[24] Altogether 102 NBC rings were found at 54°W during the 15 year period simulated with FLAME. The rings were mainly surface intensified, only 10 subsurface types were produced. Furthermore, the deep reaching types were more common than the shallow types (51 versus 41) for the surface rings. The distinction of ring types was generally straightforward, since the velocity in shallow surface rings decreases rapidly to <30 cm/s at depth below 200 m, while the deep surface types still exhibit swirl velocities >45 cm/s at 400 m depth.

[25] The average ring shedding was 6.8 rings per year in FLAME. Compared to the calculated ring shedding from observations, the model results are reasonable: In the analysis of a 10 year time series of altimeter data by *Goni and Johns* [2003], a mean ring shedding of 5–6 rings per year was estimated (of the surface intensified type only, since identified by sea surface height anomalies). However, *Johns et al.* [2003] combined ship measurements in the region 6°N–10°N off the South American continental shelf with results from moored instruments [*Garzoli et al.*, 2003]. They identified 12 surface rings and 4 subsurface rings in a period of 22 months, which yields a mean ring shedding of 8.5 rings

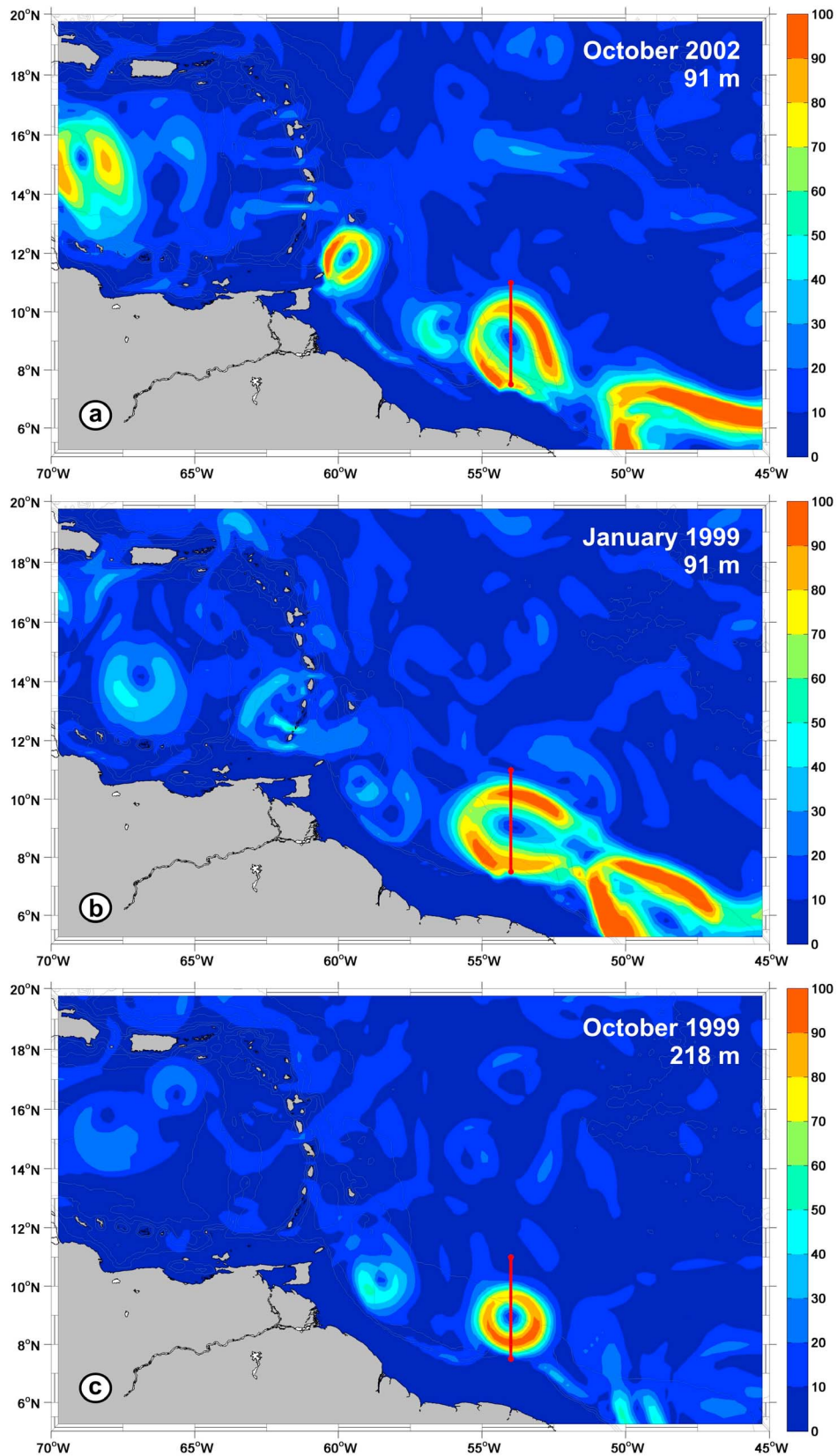


**Figure 2.** Snapshots of current speed (cm/s) for the depth levels (a and b) 91 m and (c) 218 m during October 2002 (Figure 2a), January 1999 (Figure 2b), and October 1999 (Figure 2c). The section used for the ring count at 54°W is indicated in red.

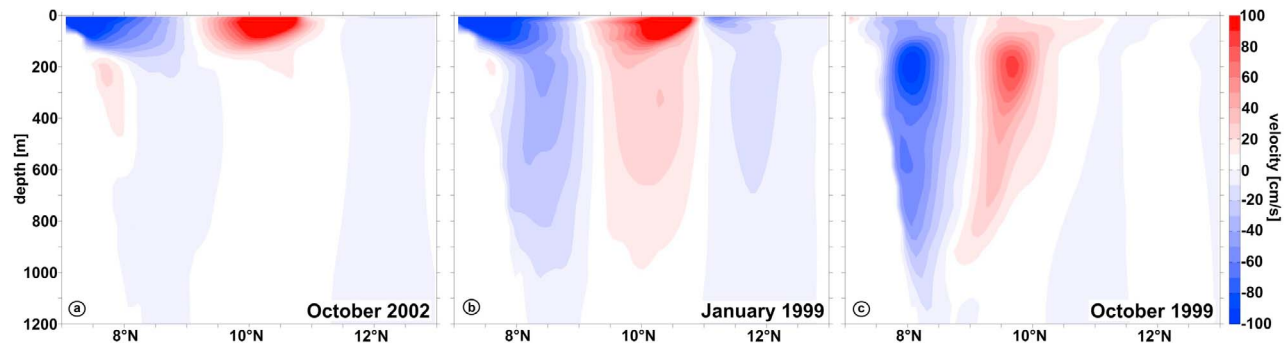


**Figure 3.** Vertical velocity structure of the NBC rings shown in Figure 2. The zonal velocity along  $54^\circ\text{W}$  is given in cm/s during (a) October 2002, (b) January 1999, and (c) October 1999.

per year. This value is somewhat higher than the model results due to the accumulated occurrence of subsurface rings (shedding rate: 2.2 rings per year). Thus considering the subsurface types a difference occurs between the observations and FLAME, where the shedding rate of subsurface rings is only 0.7 rings per year; these types are relatively uncommon in the model. Most subsurface rings occurred in 1995 (cf. Figure 5), where three of this type were produced. Note that a quantitative assessment of this model aspect is hampered by the relative short, 22 month duration of the observations: i.e., it is possible to identify a 22 month period in the model during which 4 subsurface rings are formed (1994/1995).

[26] The mean ring diameter was determined by measuring the distance from the northern to the southern outer edge of swirl velocity, since this edge was obvious in the modeled velocity and clearly the boundary of the rings. For this method the boundaries of the rings were identified as the locations, where the gradient of velocity was strongest (“gradient method” in the following). The mean diameter for surface rings was thus estimated to be  $363 \pm 59$  km in FLAME. Similar results were obtained by *Garzoli et al.* [2003], who identified NBC rings off the Brazilian coast

and calculated a mean ring diameter of 392 km from moored instruments. The satellite analysis by *Goni and Johns* [2003] reported in a mean ring diameter of only 200 km, however the ship derived measurements from *Johns et al.* [2003] lead to diameters varying from 200 to 320 km. The differences between the model and the observational estimates are probably features of the different methods to determine the ring diameter and the resolution of the observations. Using the distance from the center to the location of maximum velocity as a measure for the ring radius (as in *Goni and Johns* [2003] and *Johns et al.* [2003], “maximum velocity method” in the following), the calculated diameter is only  $304 \pm 63$  km. This is still larger than most observed ring diameters.

[27] At deeper levels the mean ring diameter in FLAME is strongly reduced. This holds for the deep surface as well as the subsurface types. The diameter at 191 m is  $238 \pm 48$  km when using the gradient method, or only  $176 \pm 60$  km when using the maximum velocity method. The reduced diameter is obvious in Figure 2 for the 218 m depth level. The surface layers often stretch toward the coast (cf. Figure 3) and cover the shelf area, but the deeper layers are forced further offshore by the bordering shelf break.

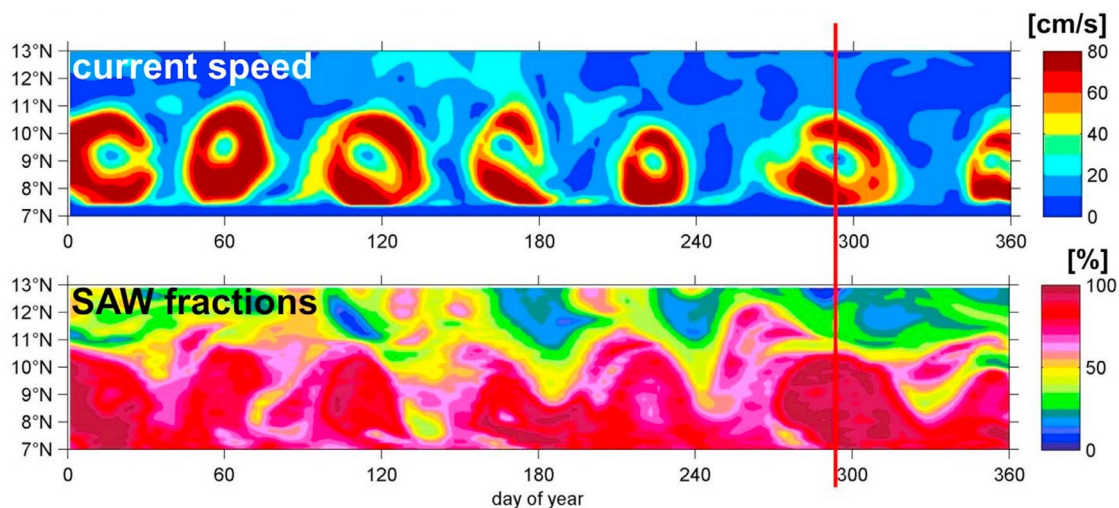


**Figure 4.** Time series of current speed (cm/s) and SAW content (%) at  $54^\circ\text{W}$  for the model year 2002 at depth level 91 m. The time of the snapshot in Figure 2a is indicated by the red line.

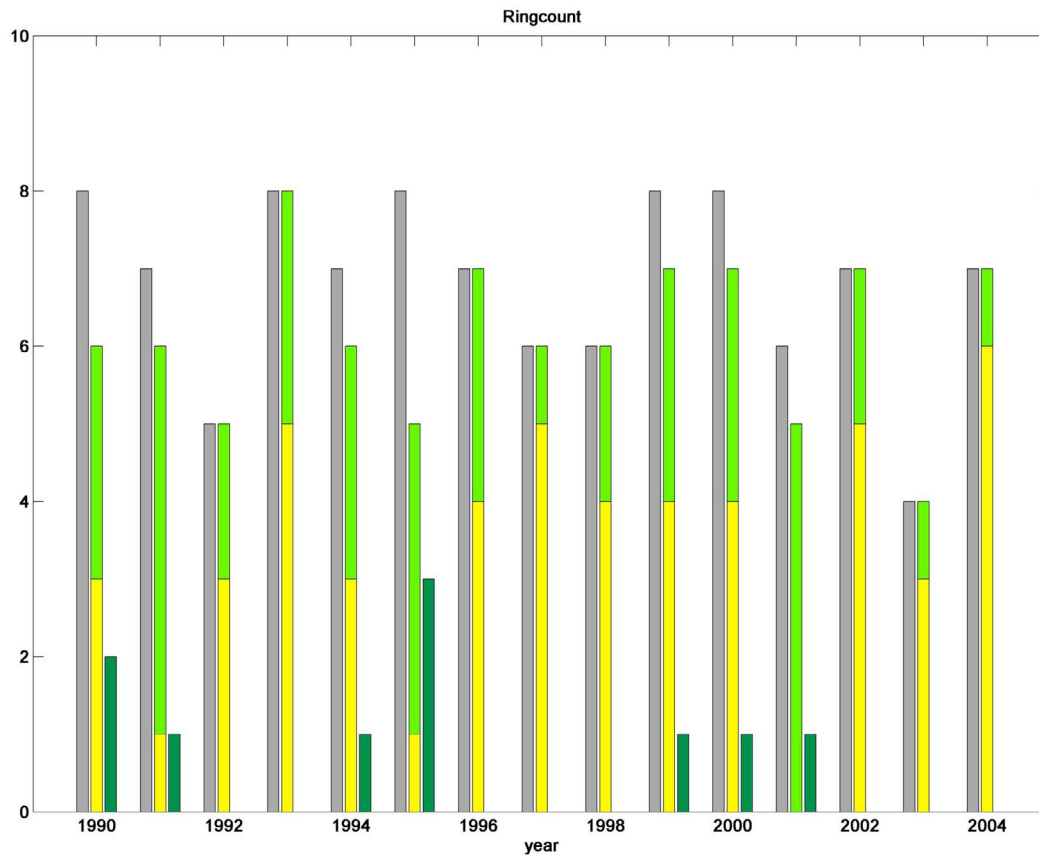


**Figure 5.** Number of rings crossing  $54^{\circ}\text{W}$  during each year in the 15 year model period from 1990 to 2004. The first bar (gray) is all rings during 1 year; the second bar (yellow) is deep, surface-intensified types; the second bar (light green) is shallow, surface-intensified types; the third bar (dark green) is subsurface-intensified types.

### 3.2. Variability in the Ring Shedding

[28] The temporal distribution of the different ring types in the FLAME time series is illustrated in Figures 5 and 6. The total ring count varies from eight to four rings per year (gray bars), but no trend is detected in the annual ring shedding in the modeled period from 1990 to 2004 (Figure 5). The occurrence of subsurface rings is scattered throughout the years, zero to three subsurface rings are produced within one year (dark green bars); the surface intensified rings are clearly the dominating ring types (yellow/light green bars). Year 2001 is the only year with no deep reaching surface ring.

[29] The seasonal ring shedding depicted in Figure 6 indicates a maximum ring production during the winter and spring periods (December–January, 28 rings; March–May, 30 rings). The ring shedding is reduced during the summer (June–August, 24 rings) and reaches a minimum in fall (September–November, 20 rings). The drop from the maximum in spring to the minimum in fall is only 30% in FLAME. In spring and summer the surface intensified rings are balanced in shallow and deep reaching types and only one subsurface type occurs in this periods. However during fall seven subsurface rings were produced and the surface intensified types changed to mainly deep reaching. The period of constantly high ring shedding from December to May

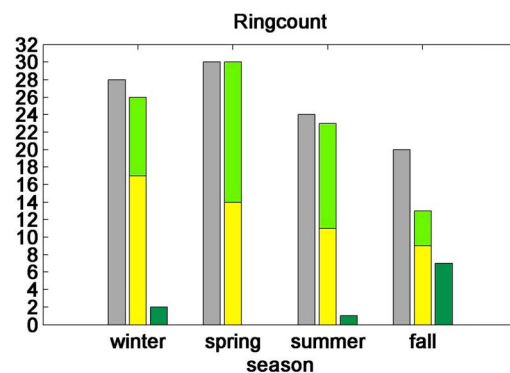


**Figure 6.** Number of rings crossing  $54^{\circ}\text{W}$  during each season (sum over the model period 1990–2004). The first bar (gray) is all rings during one season; the second bar (yellow) is deep, surface-intensified types; the second bar (light green) is shallow, surface-intensified types; the third bar (dark green) is subsurface-intensified types. Winter: December, January, February; spring: March, April, May; summer: June, July, August; fall: September, October, November.

includes the minimum strength of the NBC retroflection. This weak seasonality agrees with the results from *Goni and Johns* [2003] based on satellite altimetry, who reported a high year-to-year variability with ring shedding any time of the year, where the rings showed a weak tendency to form in the first half of the year.

[30] The detailed analysis of the ring shedding in the FLAME time series has shown, that the model reproduces the shedding of surface intensified rings realistically, both the frequency and the diameter of the rings are reasonable. However, there are indications that the model underestimates the production of subsurface NBC rings.

### 3.3. Volume Transport by NBC Rings

[31] Assuming a geometric shape of the rings, the mean volume can be calculated for all ring types. The shallow surface rings are confined to the upper 200 m, a ring of this type hence possesses a volume of  $2.1 \cdot 10^{13} \text{ m}^3$  (using the diameter from the gradient method). The deep reaching surface rings consist of an upper part, which is similar in diameter to the shallow rings, and a lower part with a reduced diameter. The subsurface part is well structured to a depth of 600 m, but below the velocity weakens to  $<20 \text{ cm/s}$  (cf. Figure 3). The combined ring volume from the surface to 600 m depth adds up to  $3.9 \cdot 10^{13} \text{ m}^3$ . The subsurface types occupy the depth range from 200 to 800 m and hold a volume of  $2.7 \cdot 10^{13} \text{ m}^3$  per ring. Considering all rings in the 15 year time series, the annualized volume transport for the rings in FLAME hence amounts to  $2.5 \cdot 10^{14} \text{ m}^3$  per year or 6.6 Sv. The obtained volume estimates and transports are clearly constrained by the diameters used for the calculations. When using the reduced diameters from the maximum velocity method, the estimated transport is only 4.4 Sv. While the first transport result accurately agrees with the annualized transport of NBC rings in MICOM, which is 6.6 Sv as well (calculated at  $10^\circ\text{N}$  in *Garraffo et al.* [2003], their Table 3), the second transport estimate of 4.4 Sv is smaller.

### 4. NBC Rings Near the Lesser Antilles

[32] In this section the downstream propagation of NBC rings toward the Lesser Antilles is investigated and the results of their interaction with the topography of the island arc are analyzed. In Figure 7 an example of the current field from April 2004 for the Lesser Antilles area is presented. Two anticyclonic vortices are apparent (indicated by the white circles), one is located around Barbados, while the other is further north near Guadeloupe/Antigua. Illustrated in the background coloring of Figures 7b–7d is the SAW content in percent. Obviously the islands bordering the Caribbean are shallow ocean points in the model topography, since the pattern of the surface currents is not deformed by the presence of the islands (Figure 7a). This circumstance reveals an important disagreement between the model and the actual ring propagation: the model probably fails in reproducing the surface ring pathways, as they can enter the Caribbean less hindered than in reality. In contrast the influence of topography is evident in the subsurface layers, restricting the westward flow into the Caribbean. The island of Barbados represents an obstacle for the northward flow. The three islands Barbados, St. Vincent and Tobago form a topographic

barrier in the shape of a triangle (Figure 1), which is capable of trapping the deeper parts of a ring. This is illustrated by the southern ring in Figures 7b and 7c: the SMW layer (Figure 7b) shows a large anticyclonic ring around Barbados (as in the surface layer), but in the UCW (Figure 7c) this ring is split into two vortices, one north of Barbados and another one located between Barbados and Tobago. The current speeds decrease with depth and in the two lowest layers only the rings are prominent features in the velocity field, which exhibit velocities  $>10 \text{ cm/s}$ ; the currents outside of rings are weak. North of St. Lucia (approximately  $15^\circ\text{N}$ ) the water masses below the SMW exhibit weak currents, and the northern ring from Figures 7a, 7b, and 7c is not identified in Figure 7d. The ring centering Barbados has a diameter of 325 km in the upper two layers, but the northern ring is slightly smaller, a diameter of 287 km is obtained. These diameters are well within the range of the observed rings.

#### 4.1. Ring Trapping at the St. Lucia-Barbados Gap

[33] The background coloring of SAW content in Figures 7b–7d shows, that the water mass analysis is a suitable tool for tracking the NBC rings. The rings do not only exhibit an anticyclonic sense of rotation in the velocity field, but high SAW contents in their center as well. Tracking is easiest done in the UCW layer, where the background SAW fraction is very small. An example for an NBC ring approaching the Lesser Antilles in this depth range is given in Figure 8 for February 2004. The ring follows the South American coastline and arrives at the islands of Trinidad and Tobago on 1–3 February (Figure 8a). The ring core is composed of more than 90% SAW, which reveals the ring clearly against the background SAW content (below 20%). The currents are strongest in the ring; it is the major signal in this velocity field. The diameter of the ring is 220 km in Figure 8a. During the following days the ring moves around Tobago and finally gets trapped between St. Lucia and Barbados at the end of February (Figures 8b and 8c). Apparently, some ring volume is lost and enters the Caribbean Sea through Grenada and St. Lucia Passage, where traces of elevated SAW fractions appear. The ring diameter decreases and at last passes northward through the gap between the two islands St. Lucia and Barbados. The passage between these islands has a width of 180 km, which is identical to the ring diameter in Figure 8d. The propagation of the ring center from  $11^\circ\text{N}$  (east of Trinidad) to  $13.5^\circ\text{N}$  (north of Barbados) has taken 40 days in the model. A week later the ring is still attached to Barbados and a new NBC ring with an SAW rich center approaches the Lesser Antilles from the south (Figure 8e). The ring north of Barbados travels around the island, finally merging with the subsequent ring, as illustrated in Figure 8f.

[34] The example presented above shows the prevailing behavior of all NBC rings in FLAME. The rings formed during the years 2003–2004 were analyzed in detail, when they approached the Lesser Antilles along the South American coastline. Within the 2 years eight rings entered the region between  $58^\circ\text{W}$  and  $61^\circ\text{W}$ . They had a diameter of 220 km at minimum and 270 km at maximum at  $11^\circ\text{N}$  (mean, 250 km). All the rings moved northwestward around Tobago and were trapped ahead of the passage St. Lucia-Barbados. Only after the rings had lost some volume to the Caribbean Sea,



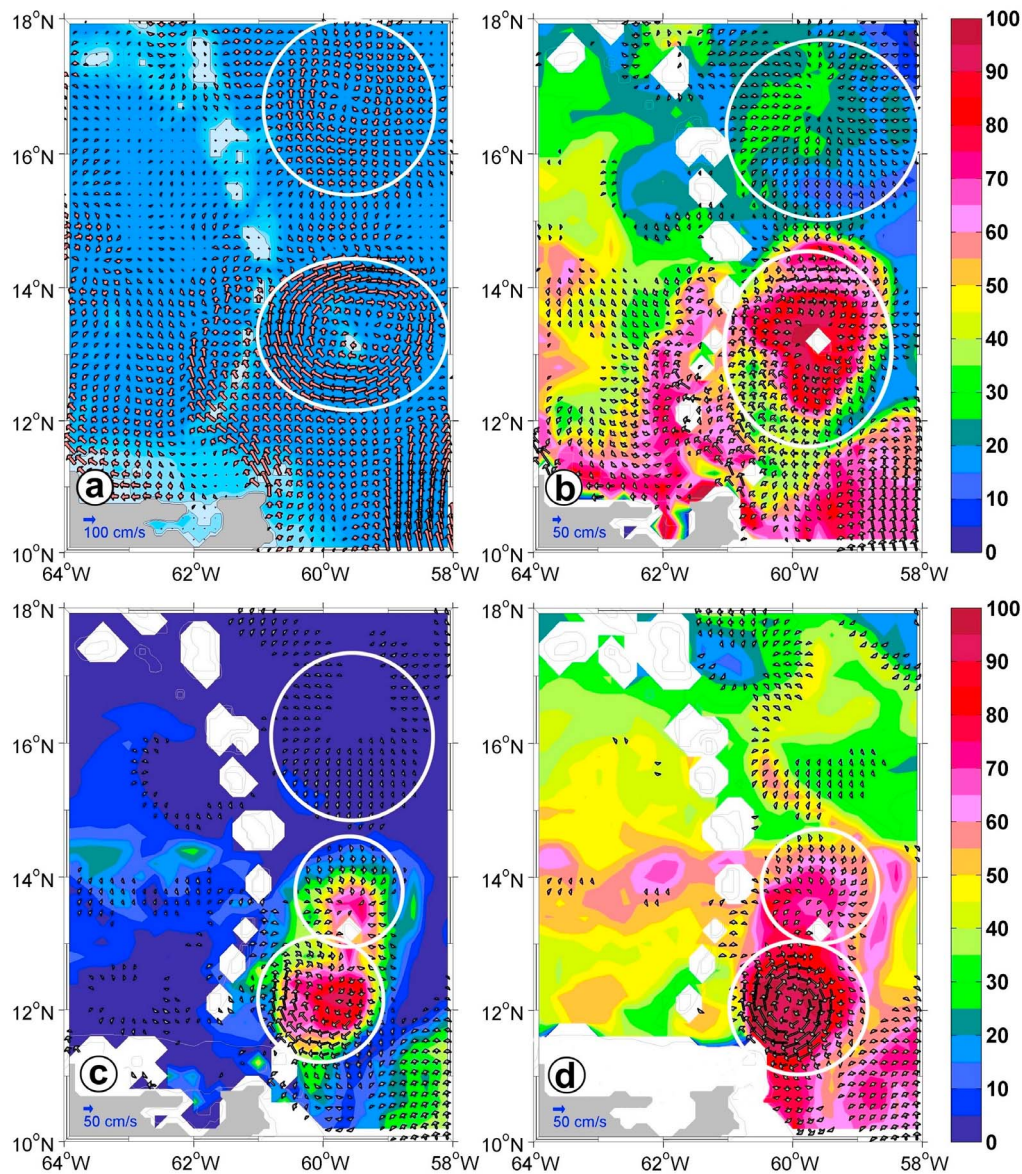


**Figure 7.** Modeled currents near the Lesser Antilles, illustrated are 3 day mean velocity vectors (arrows) in 8–10 April 2004. For clarity, only every second velocity vector is shown, when a speed of  $10 \text{ cm s}^{-1}$  is exceeded. Examples of anticyclonic vortices are framed by white circles: (a) surface layer, (b) SMW layer, (c) UCW layer, and (d) LCW layer. The background indicates the model topography (gray/white), and Figures 7b–7d indicate the SAW distribution (in %).

which reduced their diameter to 180 km, they passed through the St. Lucia-Barbados gap. Another example for the ring reduction within the topographic trap is illustrated in Figure 9 for currents in the Lower Central Water. The ring stalled in the triangle between St. Lucia, Barbados and Tobago, and only after some volume loss passed through the St. Lucia-Barbados gap (Figures 9a–9d). The remaining vortex merged with a subsequent ring and a huge anticyclone around Barbados was formed (Figures 9e and 9f). A small cyclone is noted at  $14.5^\circ\text{N}$  (see below).

[35] The water imported into the Caribbean Sea by the reduction of ring volume within the island triangle carries a strong SAW signature. The flow is very restricted and jet-like, since the Lesser Antilles Passages are much smaller

than the 180 km width of the St. Lucia-Barbados section. The rings do not enter the Caribbean as vortices. Interaction with the islands nevertheless leads to the formation of new rings in the eastern Caribbean, when the currents in the passages are strong enough (observed by drifter trajectories [Richardson, 2005]; observed by laboratory experiments [Cenedese *et al.*, 2005]). The deeper parts in an NBC ring undergo a similar transformation to smaller vortices due to interaction with the topography of the Lesser Antilles island arc. The upper layers in contrast feature larger rings, which are at minimum 220 km and at maximum 380 km in diameter and not influenced much by the presence of the Lesser Antilles due to the imperfect model topography (see section 2).

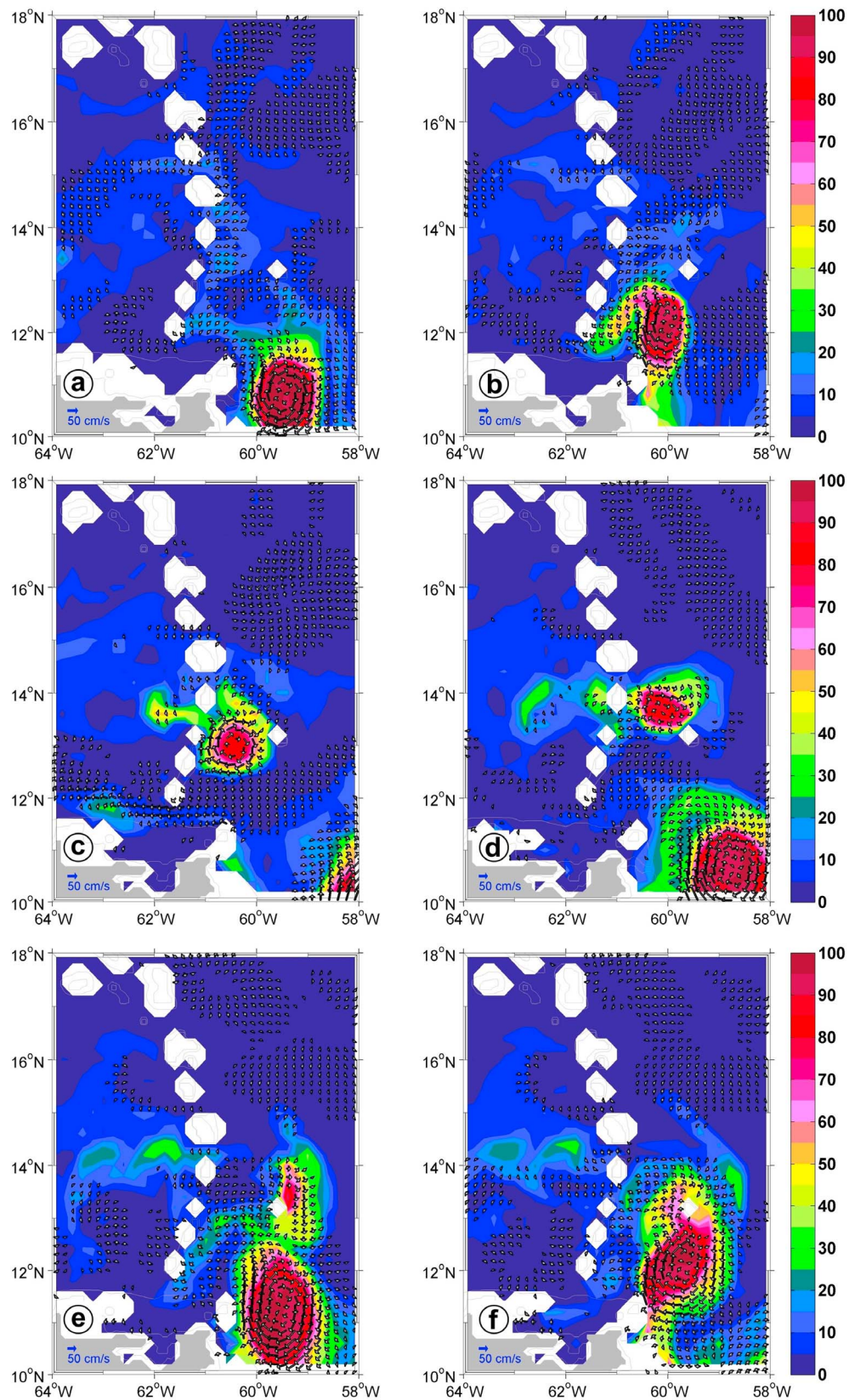


**Figure 8.** Modeled currents near the Lesser Antilles in the UCW layer with SAW content in the background. For clarity, only every second velocity vector is shown, when a speed of  $10 \text{ cm s}^{-1}$  is exceeded. The Figures show 3 day means in 2004: (a) 1–3 February, (b) 10–12 February, (c) 25–27 February, (d) 12–14 March, (e) 24–26 March, and (f) 30 March to 1 April.

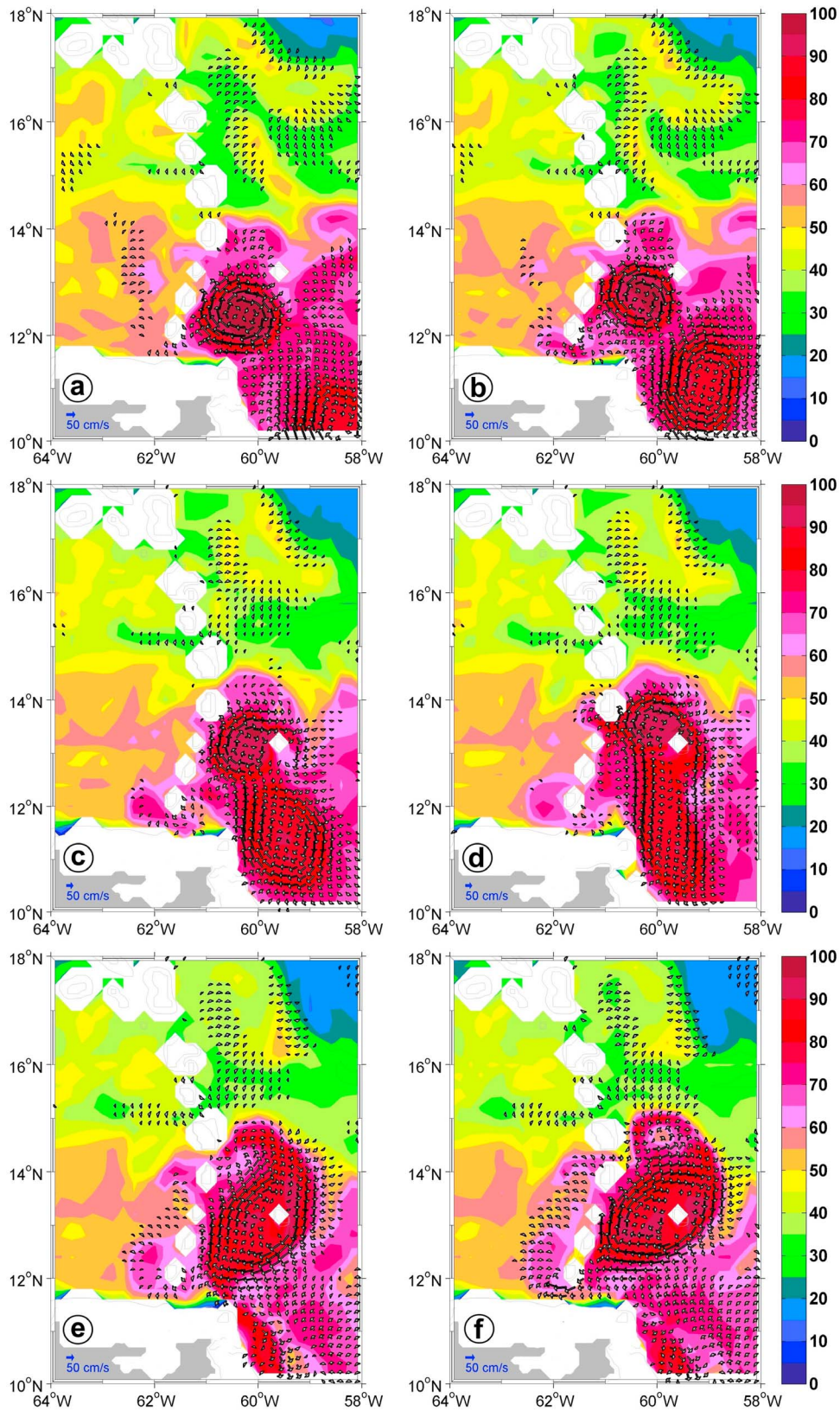


**Figure 9.** Modeled currents near the Lesser Antilles in the LCW layer with SAW content in the background. For clarity, only every second velocity vector is shown, when a speed of  $10 \text{ cm s}^{-1}$  is exceeded. The Figures show 3 day means in 2003: (a) 25–27 January, (b) 31 January to 2 February, (c) 6–8 February, (d) 9–12 February, (e) 16–18 February, and (f) 19–21 February.

#### 4.2. Consequences of Ring-Topography Interaction and the Formation of New Eddies

[36] A common behavior after the ring reduction near St. Lucia and Barbados is the passing of the remaining vortex through the gap, followed by a circular motion of the ring remnant around Barbados. The island remains located on the right side of the moving vortex, even though they eventually move southeastward again. The old vortices then merge with subsequent rings, as was illustrated in Figures 8 and 9. Most of the rings do not “survive” the passage through the St. Lucia-Barbados section and disintegrate in the island triangle. Streams separate from these rings, and parts of the streams continue northward along the island arc, contributing to the transport through Dominica and Guadeloupe Passage. Other parts of the streams shape clockwise around Barbados, forming large rings with Barbados in the center as shown in Figure 9. Anticyclonic flow around Barbados occurs in all depth layers to 1100 m. Eventually, new vortices are formed by the streams north of 14°N. The newly formed eddies carry a less significant SAW structure than the original NBC rings found at 11°N. Their diameters do not exceed 200 km.

[37] Occasionally cyclonic eddies are produced in FLAME north of Barbados as a result of the interaction with topography. An example is presented in Figure 10 for March 2003, where the eddy is highlighted by white circles. A distinct core, containing a noticeable amount of SAW, is visible in the subsurface layers, as well as cyclonic currents in the velocity field at all depth levels. The cyclone has a diameter of approximately 180 km. The swirl velocity however is weaker than in original NBC rings south of Barbados (especially in the surface currents) and the SAW contained in the core of the eddy is diluted. Most obvious is again the UCW layer: rings south of Barbados contain 90% SAW in their core (cf. Figure 8), but the SAW fractions in the newly formed cyclone stay below 40%. A small cyclone was also noted in Figure 9f, centered at 14.5°N. The small cyclone contained less SAW than the original NBC rings as well.

[38] Results from laboratory experiments correspond to the behavior of NBC rings near the Lesser Antilles in FLAME. *Cenedese et al.* [2005] described several experiments in a rotating tank, where they produced a cyclonic vortex and examined the interaction of the westward moving vortex with two cylindrical obstacles. When a large vortex encountered the smaller gap between two cylinders, the original vortex was unable to move undisturbed through the gap. The authors reported the vortex to either lose most of its fluid (into a streamer through the gap) until it was able to move through the gap, or to totally disappear upstream of the gap (or move around the cylinders). In the wake of the cylinders, the streamer was able to form new vortices, which were undisturbed by the movement of the original vortex. They therefore moved on as new independent structures. Sometimes, parts of the original vortex fluid built up a stream around one cylinder, which formed a new cyclonic vortex in the wake of the cylinder. Meanwhile, the fluid of the jet moved through the gap and started forming a dipole structure downstream of it, with one cyclone and one anticyclone. The new anticyclonic vortex was stable and visible downstream of the cylinders, when the jet through the gap had sufficiently high velocity. Elevated velocities in the gap and

high Reynolds numbers were found to be necessary for the dipole production. The conclusions from *Cenedese et al.* [2005] are not limited to cyclonic vortices: one can transfer their findings to an anticyclonic vortex by changing the sign of swirl velocity. The authors predicted a clockwise movement of anticyclonic vortices around an obstacle, corresponding to the case of a ring circling around Barbados, as in Figures 8 and 9.

[39] A direct comparison between the laboratory experiment and observations of drifter trajectories is provided by *Cenedese et al.* [2005] and adopted with extensions here in Figure 11. In Figure 11a drifter trajectories from *Fratantoni and Richardson* [2006] are illustrated. One of the drifters started a cyclonic loop approximately 300 km downstream of Barbados, which is near the latitude of Guadeloupe. The tank experiment in Figure 11b presents the interaction of a cyclonic vortex with a gap between two islands: a stream is formed anticlockwise around the right cylinder (thin line), and a dipole with one cyclone and one anticyclone develops downstream of the islands (thick line, dashed line). As the NBC rings are anticyclonic vortices, the directions of the resulting currents after interaction with Barbados and St. Lucia is reversed: a stream would enter the gap and move around the right cylinder in clockwise direction (as described in FLAME, see above) and no northward flow occurs to the east of the islands. The cyclone would develop at the right side of the dipole. This is consistent with the observations described by *Fratantoni and Richardson* [2006]. In Figure 11c the trajectories of two artificial floats in FLAME are depicted (a description of the float experiment in FLAME follows in the next section). Their pathways are similar to the drifter trajectories in Figure 11a: They approach the Lesser Antilles within an anticyclonic NBC ring, pass through the Barbados-St. Lucia gap and resume looping north of Barbados. The red trajectory shows cyclonic looping and the blue trajectory shows anticyclonic looping north of Barbados.

[40] The movement of NBC ring remnants around Barbados, as well as the formation of new cyclones and anticyclones north of Barbados, was reproduced in FLAME, as expected from the laboratory experiments. The northward propagation of NBC rings is generally strongly hindered by the Lesser Antilles (particularly by Barbados) and a loss of volume occurs. No undisturbed rings are found north of the St. Lucia-Barbados Passage in the model.

#### 5. Propagation Pathways and the Fate of the Ring Cores

[41] The propagation pathways and the fate of the core waters of all ring types are investigated and discussed in this section. A useful tool for tracking the NBC rings in the model is a Lagrangian analysis with artificial floats. The floats were inserted into cores of NBC rings and integrated forward in the modeled velocity field. The starting points of the floats were located at the 54°W section, at a time when a ring was present at the section. In every calculation 1000 floats were released and their trajectories computed for the following 12 months. The analysis of the trajectories was restricted to the floats within a ring. The depth range from 60 to 385 m was used for the launching of the floats, since the model topography misses the surface parts of the

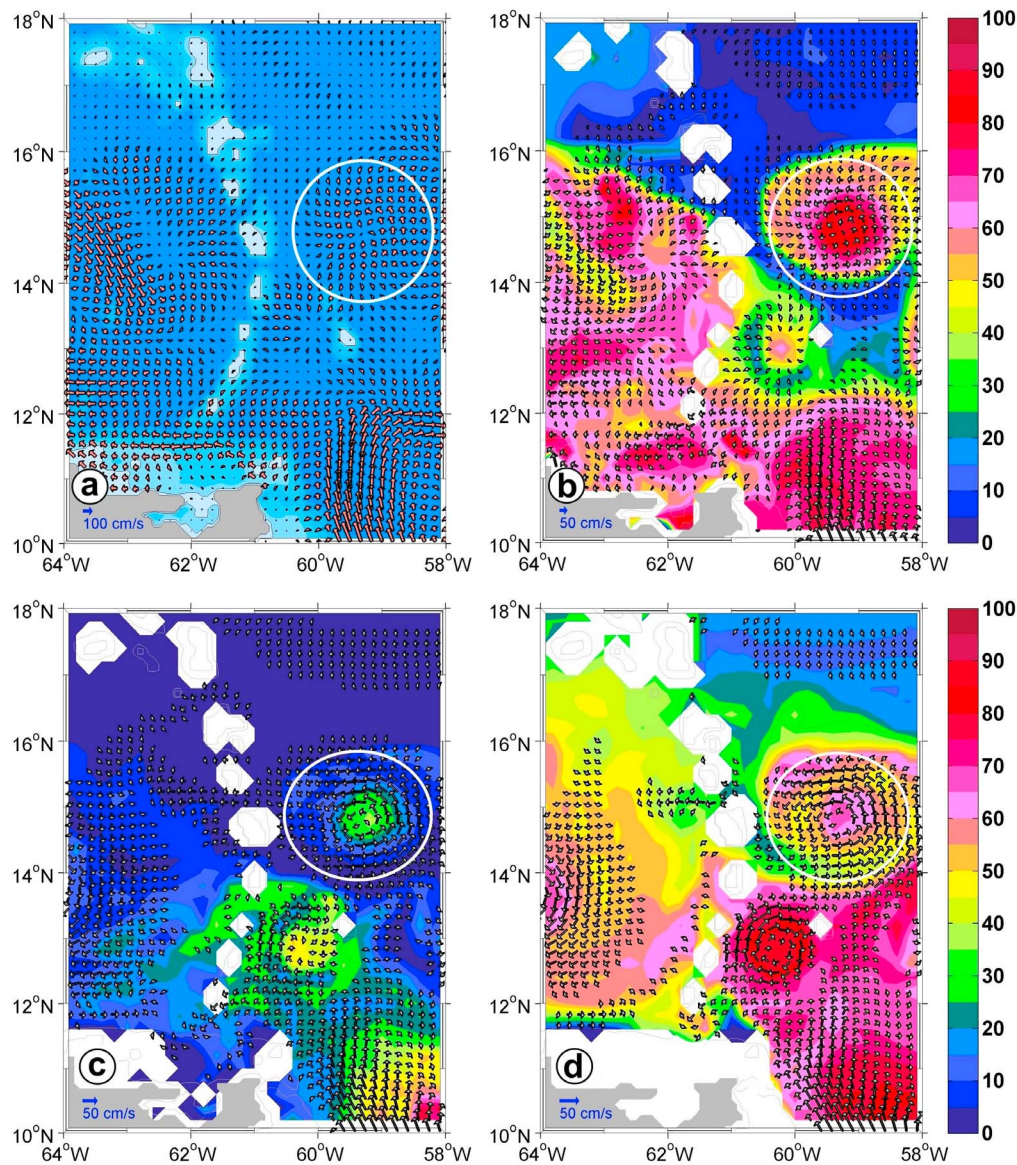


**Figure 10.** Modeled currents near the Lesser Antilles, illustrated are 3 day mean velocity vectors (arrows) in 11–13 March 2003. The cyclonic vortex is framed by white circles: (a) Surface layer, (b) SMW layer, (c) UCW layer, and (d) LCW layer. The background indicates the model topography (gray/white), and Figures 10b–10d indicate the SAW distribution (in %).

islands (see section 2). For shallow, surface intensified rings only floats to 200 m depth were considered. Within the subsurface rings floats were only launched from 190 to 385 m.

[42] The obtained trajectories were classified according to their pathway: one group entered the Caribbean Sea and crossed the longitude of 64°W, another group followed a northward pathway and crossed the latitude of 16°N near Guadeloupe in the Atlantic. A considerable amount of floats stayed in the Atlantic, not crossing 16°N nor entering the Caribbean. In Figure 12 the trajectories for the first two groups obtained from the subsurface ring in October 1999 are depicted (the sections for classifying the floats are indicated in green). In Figure 12a all float trajectories entering the Caribbean and crossing 64°W are illustrated (488 floats). The

floats use the southern passages excessively, whereas north of 15°N very few floats enter the Caribbean. This behavior agrees with the results from *Kirchner et al.* [2009], who analyzed the South Atlantic Water inflow into the Caribbean and found the northern passages of minor importance. The float trajectories crossing 16°N are presented in Figure 12b (149 floats). The trajectories indicate that many floats, which were originally taking the Atlantic pathway and crossed 16°N, performed southward loops. Some actually entered the Caribbean Sea, whereby all passages were used. Some of these floats were thus counted in the Caribbean group as well; the groups are not disjunctive. After the 1 year of calculated float drift, only 86 floats were positioned north of 16°N in the Atlantic. So even for subsurface intensified rings, as the example above, the Caribbean pathway is more

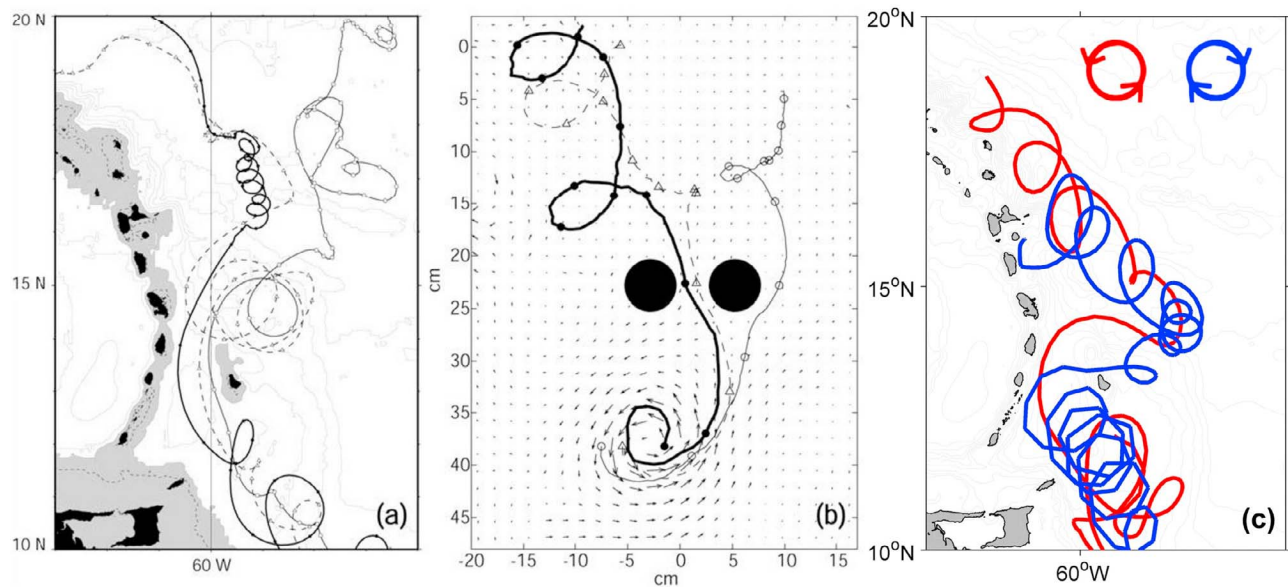


**Figure 11.** Examples of drifter trajectories near the Lesser Antilles, adopted and extended from [Cenedese *et al.*, 2005, Figure 14], for a case in which a dipole was observed downstream of an island passage. (a) Observed trajectories of three satellite-tracked surface drifters from Fratantoni and Richardson [2006], which were launched in an NBC ring in February 1999. (b) Trajectories of three synthetic drifters deployed in the velocity field of the laboratory model. Note that the sense of rotation for the laboratory eddies is reversed (cyclonic) relative to the observed anticyclonic NBC rings. (c) Two trajectories from artificial floats in FLAME are shown, which approach the Lesser Antilles within an anticyclonic NBC ring, but loop within a cyclone (red) and an anticyclone (blue) north of the passage Barbados-St. Lucia, similar to the floats in Figure 11a.

effective in FLAME. All trajectories stay in a broad channel from the  $54^{\circ}\text{W}$  section to the Lesser Antilles, few detours from this path occur. The vertical starting positions of the two different float groups depicted in Figure 12 are illustrated in the upper right corner. They show a cutout from Figure 3c, where the starting points of the floats shown in the main Figure were inserted in yellow. No regularity is evident in the starting positions for both groups, the floats are scattered throughout the whole ring core. Hence ring core water is likely leaking off the ring near the Lesser Antilles, then entrained in the surrounding currents and streamers and transported either into the Caribbean (main pathway) or northward through the St. Lucia-Barbados gap.

[43] The float calculation was performed for eight subsurface rings and 26 surface intensified rings, 12 of them deep reaching. The obtained trajectories were classified as stated above. The Caribbean group (crossing  $64^{\circ}\text{W}$ ) held 75% of the floats for the shallow, surface rings and 64% for the deep surface types. Of the floats launched in subsurface rings only 44% reached  $64^{\circ}\text{W}$  in the Caribbean. The  $16^{\circ}\text{N}$  pathway however is frequented mainly by floats from subsurface rings, but even for this ring type only 22% of all trajectories crossed  $16^{\circ}\text{N}$ . Of the floats in shallow and deep surface rings 8% and 10% reached this latitude in the Atlantic. For all rings the end position of the floats after 1 year was most often in the Caribbean Sea, south of  $16^{\circ}\text{N}$ . The differences were only small: 56% of the floats in shallow and 53% of the floats in deep surface rings terminated in this area, and 51% of the floats in subsurface rings as well. The floats remaining in the Atlantic south of  $16^{\circ}\text{N}$

varied from 20% and 27% for shallow and deep surface rings to 34% for the subsurface rings. After one year of integration, they had left their ring cores or the cores had decayed and the floats neither entered the Caribbean nor crossed  $16^{\circ}\text{N}$ . These floats may be swept into the Caribbean (or northward along the island arc) by subsequent rings during later years, but they cannot be associated with NBC ring cores anymore.

[44] A detailed inspection of the float trajectories revealed all features expected from the analysis of the current field near the topographic barrier of the Lesser Antilles above. Examples for different float trajectories are presented in Figure 13. The upper row with Figures 13a and 13b focuses on the Caribbean Sea, where the trajectories with both anticyclonic (Figure 13a) and cyclonic (Figure 13b) loops are found. This is in agreement with Cherubin and Richardson [2007], who noted the occurrence of Caribbean cyclones and anticyclones in the MICOM simulation. In Figures 13c and 13d two floats with long residence near Barbados are depicted. The float in Figure 13c loops anticyclonically around Barbados and ends near the southern passages of the Lesser Antilles. The float in Figure 13d takes a route into the Caribbean, but stalls for some time in the island triangle of St. Lucia, Barbados and Tobago. The last row shows different trajectories crossing  $16^{\circ}\text{N}$  in the Atlantic. The float in Figure 13e takes the passage between St. Lucia and Barbados swiftly. North of Barbados this float performs cyclonic loops, similar to those found in the observations by Fratantoni and Richardson [2006], presented in Figure 11. Figures 13f and 13g show examples for floats crossing

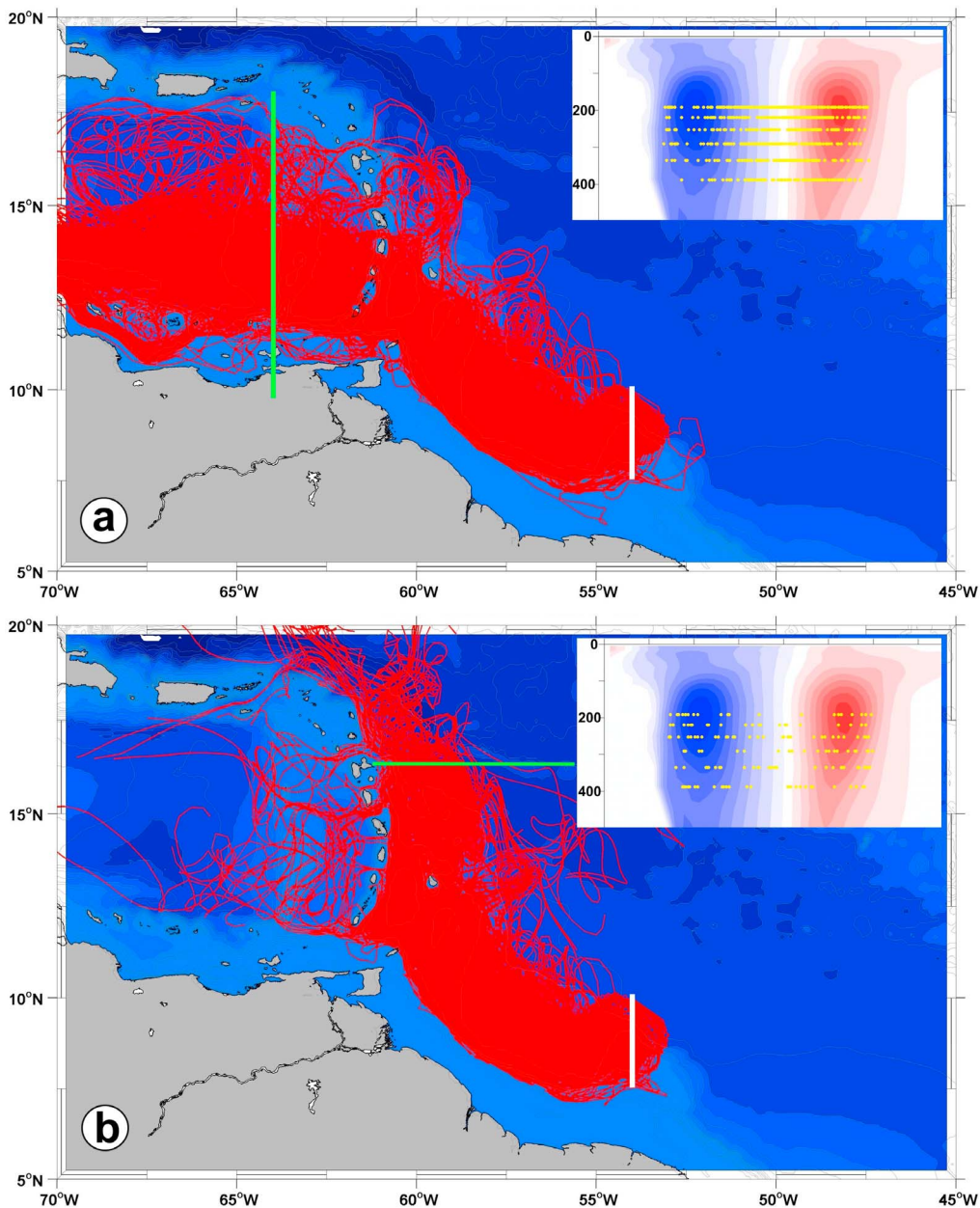


**Figure 12.** Examples of drifter trajectories for artificial floats in FLAME, inserted into a subsurface ring in October 1999. Trajectories are shown for (a) all floats crossing 64°W (green line) and (b) all floats crossing 16°N (green line). The starting points are located at 54°W (white lines). The insets show a cutout from Figure 3c, where the starting points of the floats were inserted in yellow.

16°N, but then turning south again and entering the Caribbean. The float in Figure 13g shows anticyclonic movement north of Barbados.

## 6. Summary and Discussion

[45] This study analyzed the production, propagation and decay of NBC rings in the high-resolution ocean model FLAME. The rings represent prominent high-velocity events with an anticyclonic sense of rotation in the current field. In the 15 year time series simulated with FLAME 102 NBC rings were identified at 54°W. Subsurface types were

uncommon (only 10), but most rings were of the deep reaching surface intensified type (51 deep versus 41 shallow). The average ring shedding rate was estimated to be 6.8 rings per year in the model. The mean ring diameter was  $363 \pm 59$  km near the surface and  $238 \pm 48$  km at deeper levels when using the maximum velocity gradient as criteria for the ring size. A pronounced velocity core was usually found, with mean current speeds of 90–100 cm/s above the thermocline. The temporal distribution revealed no trend in the ring shedding over the 15 year period, but a weak seasonality with a maximum of ring production in spring and a minimum in fall. The deep, surface intensified

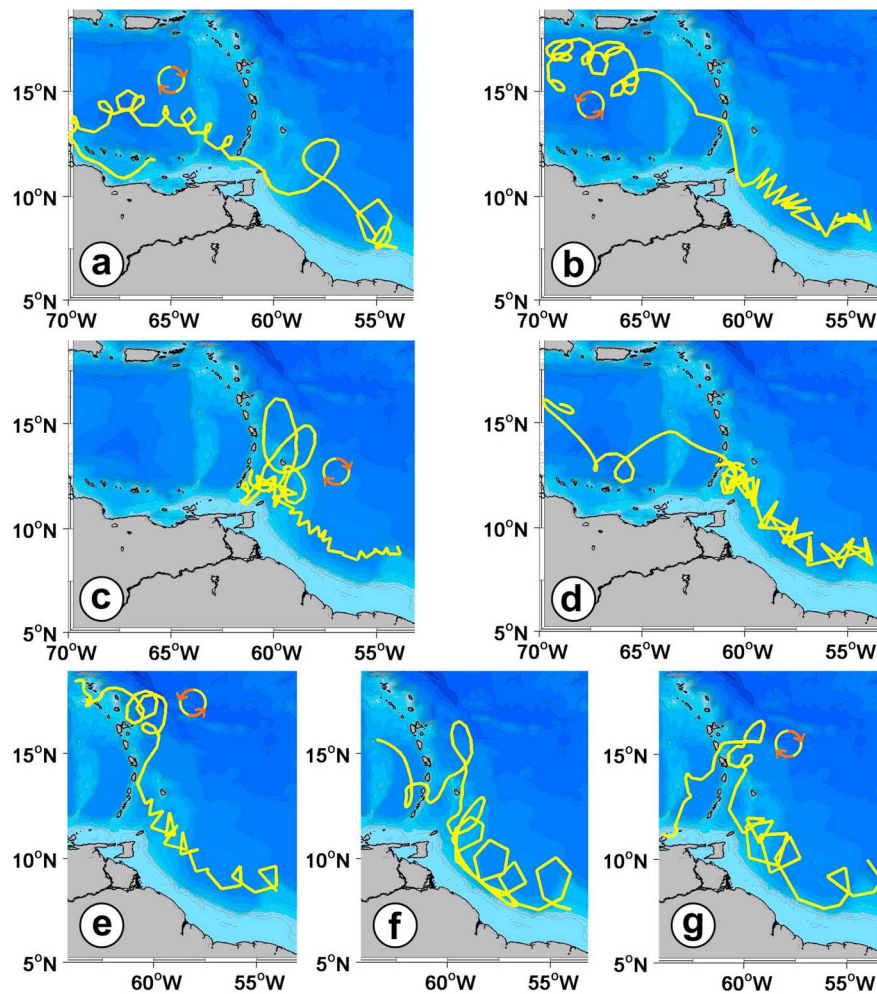


**Figure 13.** Examples of drifter trajectories for artificial floats in FLAME, which show the typical behavior of the floats as described in the text. The sense of rotation is indicated by the schematic ring (orange and yellow arrows).

rings dominate in winter and spring, but balance with shallow types in summer and fall. The subsurface rings were predominantly formed during fall. A connection with the strength or position of the NBC retroflection is not obvious. The northernmost position of the retroflection is reached during September to February, where two different periods of ring formation were found. The transport of the retroflection is strongest in July to December, which may cause the reduced shedding in fall, but in December the ring shedding is strong again.

[46] The rings in FLAME represent much stronger features in the velocity field than in earlier model studies. In the work of *Garraffo et al.* [2003] the isopycnic MICOM model was used to analyze the ring shedding and structure. The rings in MICOM typically show velocities smaller than 80 cm/s in the ring cores and diameters of 240 km for the surface intensified types and 164 km for the subsurface types. Compared to the rings in FLAME, where surface diameters of 304 km and subsurface diameters of 176 km were obtained by the same method using the maximum swirl velocity, the MICOM model run thus produced smaller and weaker rings especially in the surface layer. FLAME matches

the upper limit of the observed rings in diameter and strong currents of O (100 cm/s), similar to the observed velocities in the work of *Johns et al.* [2003]. Both models agree on the accumulation of subsurface rings in the fall period and the dominance of shallow surface rings in summer. Though a difference occurs in the shedding rate: in FLAME only 0.7 subsurface rings per year are produced, while MICOM generates two subsurface types per year. The observations are so far too sparse to dissolve this discrepancy, since no long-term time series exists in the subsurface layer.

[47] The FLAME results however indicate a ring shedding maximum in December–May, which is in agreement with the observed surface rings in the work of *Goni and Johns* [2003], while MICOM shows a distinctive maximum in May. The seasonality is much less pronounced in FLAME, where all ring types are found all year-round. In summary, the results presented here using FLAME show a better agreement with recent observations than the MICOM analysis, which is probably a consequence of the different model setup in FLAME. The forcing was different in the two models (monthly climatology from COADS in MICOM, daily NCEP/ECMWF in FLAME), as well as the boundary



conditions. In addition the MICOM model used isopycnic layers, whereas FLAME was run on  $z$  coordinates.

[48] Nevertheless both models reveal comparable annualized volume transports by NBC rings. The MICOM analysis resulted in a transport of 6.6 Sv, while the FLAME estimate is 4.4 Sv when using the same method for defining the ring radii (maximum velocity criteria). If the larger diameters obtained by the velocity gradient methods are used, the ring transport in FLAME increases to 6.6 Sv. These calculations of the FLAME ring transports represent lower estimates, since the vertical extension of the deep surface rings was assumed to be only 600 m. An upper estimate is obtained by using 900 m as the lower boundary of deep surface rings and 1000 m for the subsurface rings: the transport increases to 5.1 Sv (maximum velocity method) and 8 Sv (gradient method). *Garraffo et al.* [2003] pointed out, that when using a water mass analysis for calculating the ring volumes (rather than the swirl velocity), a larger diameter and thus larger transports are obtained. The results in MICOM yielded a 15% increase in transport (from 6.6 to 7.5 Sv) when the SAW content defined the ring boundaries, which agrees well with the transports obtained in FLAME using the gradient method (6.6–8 Sv). The modeling results correspond to the findings in *Kirchner et al.* [2008], who reported an inflow of 8.6 Sv South Atlantic Water into the Caribbean, and to the analysis of a 18 month time series from mooring data by *Garzoli et al.* [2003], who revealed a mean transport of 8 Sv by NBC rings. Considering the overturning stream function, which amounts 16 Sv in the tropical Atlantic in FLAME [*Kirchner et al.*, 2008, their Figure 6], the NBC rings account for 40%–50% of the meridional transport. *Johns et al.* [2003] used various observations and determined an annualized ring transport of 9.3 Sv, which represents more than 50% of upper ocean MOC transport. Nevertheless, the observed time series are still short and may be biased by seasonal and/or interannual variability.

[49] We conclude that FLAME is able to reproduce the vertical structure and the shedding of NBC rings with sufficient accuracy. Subsurface types were found to be nearly unimportant (which may be erroneous), but deep surface intensified types were most frequently produced. An impetuous interaction of the rings approaching the Lesser Antilles is therefore expected, since the shoaling topography at the narrow passages is particularly acting on the deeper levels of the rings.

[50] The interaction of NBC rings with the topography of the Lesser Antilles was investigated in the small region 10°N–18°N, 58°W–64°W. Thereby a water mass analysis was found to be a useful tool, as the tracking of the rings was easily done when combining the SAW distribution in the Central Water with the velocity field. The surface currents are not influenced by the presence of the Lesser Antilles in FLAME, due to inaccuracies in the model topography. Thus the surface layer could not reproduce the real ring propagation and was left out in this work. The rings approached the Lesser Antilles from the southeast, moved northward around Tobago and were trapped in the topographic triangle of Tobago, St. Lucia and Barbados. They stayed at this position until their diameter was reduced to approximately 180 km, finally passing through the St. Lucia–Barbados gap. Some of the rings did not continue their path northward, but

disintegrated totally at this topographic trap. The volume export from the rings occurred by streamers or jets, which either entered the Caribbean Sea, or migrated clockwise around Barbados or flowed northward on the eastern side of the island arc. Occasionally the streamers formed new vortices with subsequent NBC rings around Barbados, or new anticyclonic and sometimes cyclonic vortices north of Barbados. These results are consistent with observed drifter trajectories, e.g., *Fratantoni and Richardson* [2006] described clockwise movements of drifters around Barbados and both anticyclonic and cyclonic loops north of Barbados. The modeling results from *Simmons and Nof* [2002], who suggested that NBC rings are likely to enter the Caribbean Sea as coherent structures, were not confirmed in the FLAME analysis. The cause for this discrepancy is likely the different model setups and the modeled topography. While *Simmons and Nof* [2002] modeled the interactions of zonally propagating eddies with a meridional wall containing gaps, in the FLAME model the complex passages of the Lesser Antilles are used and the NBC rings are moving northwestward. Nevertheless the second conclusion in the work of *Simmons and Nof* [2002] of a breakup of NBC rings after collisions with Grenada and the Grenadines was reproduced.

[51] An analysis of artificial floats in FLAME was used to investigate the pathways of the rings and the fate of the ring cores. The floats were inserted into the modeled velocity field, directly into several ring cores. The propagation of the floats from the starting points (at 54°W) near the ring shedding region toward the Lesser Antilles is confined to a corridor of 250 km width, which is following the coastline. The vast majority of the floats stays in this path, until the topography of the Lesser Antilles disturb their propagation. Different groups of floats were classified for the region north of Trinidad (approximately 11°N), where their propagation was hindered by the complex topography of the Lesser Antilles. The majority of the floats entered the Caribbean (75% versus 64% in the shallow and deep surface rings, 44% in the subsurface rings). The northward, Atlantic pathway was found to be of minor importance, and many floats crossing 16°N east of Guadeloupe recirculated southward again. Of the floats turning northward at Tobago, most squeeze through the St. Lucia–Barbados gap. No prominent pathway was found east of Barbados, where a ring could avoid the interaction with the islands and migrate toward the northern Lesser Antilles undisturbed.

[52] *Fratantoni and Richardson* [2006] suggested a separation of rings at 200–400 m, in an upper and a lower part, at the latitude of Tobago. The shallow part was found to propagate further northwestward, while the deeper part remained near Tobago, interacting with subsequent rings. Ring-ring interactions were found to be commonplace by *Fratantoni and Richardson* [2006]. The model exhibits frequent ring-ring interaction as well, but the separation of rings in two parts could not be validated in the FLAME analysis at this latitude. The deep part of the rings rather stalls in the topographic trap north of Tobago. The shallow surface rings were found to transport most of their core into the Caribbean in the floats analysis, a northward propagation is thus more advanced in the deep and subsurface rings.

[53] Although the influence of the Lesser Antilles on the NBC rings was found to be complex, the presented con-

sequences of interaction with the islands corresponded well to the results of laboratory experiments from *Cenedese et al.* [2005]. The import into the Caribbean from the reduction of the ring volume at the Lesser Antilles probably follows the same mechanisms. The streams passing through the Lesser Antilles island passages eventually induce new ring formation, since both anticyclonic and cyclonic loops were found in the float trajectories, analogue to observations in the eastern Caribbean Sea as well [Richardson, 2005]. High eddy activity in the Caribbean Sea is equally indicated by Argo trajectories. Richardson [2005] and Fratantoni and Richardson [2006] described cyclones north and east of the Leeward Islands from drifter trajectories. Fratantoni and Richardson [2006] even connected the apparent cyclone north of Barbados with the accelerated flow through the St. Vincent-Barbados gap. The observed cyclonic vortex drifted northward along the island arc. The modeling results presented in this work are very similar.

[54] The observations by Rhein et al. [2005] at 16°N revealed the existence of NBC rings along the section, which could be identified in the SAW distributions and velocity field. All rings encountered during their ship cruises were found to be deep reaching, but both surface and subsurface intensified types occurred. Although the diameter at 16°N was 230 km for the surface rings, hence reduced when compared to the size near the ring formation, the vertical structure was still conserved. This indicates some volume loss from the rings along the way, but no intense topographic interaction that would deform the ring composition thoroughly. Only for the ring found in June 2003 at 16°N the velocity field indicates a cyclone, rather than an original NBC ring as formerly assumed in the work of Rhein et al. [2005, their Figure 7d]. When considering the model results presented here, a cyclone found in the observations becomes a possible feature, formed as a result of NBC ring interaction with the St. Lucia-Barbados gap. The model analysis revealed no suitable pathway to achieve this relatively undisturbed propagation of NBC rings to 16°N. In the model all rings moved toward the Lesser Antilles, interacted with the islands and altered their size and structure. Only smaller vortices with reduced SAW content were found north of the St. Lucia-Barbados gap, which were either NBC ring remnants or newly formed vortices. The investigation of NBC rings in FLAME has thus provided two mechanisms for water from the ring cores to reach the latitude 16°N off Guadeloupe: firstly, NBC rings can approach the Lesser Antilles from the southeast, interact with the islands and be reduced to small vortices (approx. 180 km in diameter) when reaching 16°N. Secondly, rings may take the same pathway, but disintegrate at the islands into streamers and new eddies (anticyclonic and cyclonic) are formed out of streams north of Barbados which propagate to 16°N. This newly-formed rings have a deformed SAW core and a less pronounced maximum in SAW due to mixing with the waters north of Barbados. The growing data set of the Argo project and the Global Drifter Project will be useful to provide further validation of the model results (<http://argo.jcommops.org/>, <http://www.aoml.noaa.gov/phod/dac/dacdata.html>).

[55] Finally we give the answers to the initial motivating questions in the introduction: (1) The study has shown that the high resolution ocean model FLAME is able to reproduce the vertical structure and behavior of the NBC rings. (2) The

subsurface types represent only 10% of all rings shed, but 50% are of the surface, deep reaching type. (3) The interaction with the Lesser Antilles leads to the decay of the rings, new Caribbean Eddies or Atlantic cyclones and anticyclones may form as a consequence. No undisturbed pathway to 16°N was found in the model. (4) The core water from subsurface rings reaches more often the latitude of 16°N than the water from surface rings, but the Caribbean pathway is most important for all ring types. (5) The annualized cross hemispheric ring transport ranges between 4.4 Sv and 8 Sv, depending on the methods used to calculate the ring radii and volumes.

[56] **Acknowledgments.** We thank Silvia Garzoli and an anonymous reviewer for their helpful comments and suggestions to improve the quality of this manuscript. We acknowledge the contributions of J. Dengg, R. Redler, J.-O. Beismann, C. Eden, and L. Czeschel to the FLAME development and integration. The computations were performed at DKRZ, Hamburg. Financial support was received by the Deutsche Forschungsgemeinschaft (DFG grant JO 809/1-1).

## References

- Arakawa, A. (1966), Computational design for long-term numerical integration of the equations of fluid motion: Two-dimensional incompressible flow. Part 1, *J. Comput. Phys.*, *1*, 119–143.
- Barnier, B., L. Sieffridt, and P. Marchesio (1995), Thermal forcing for a global ocean circulation model using a three year climatology of ECMWF analysis, *J. Mar. Syst.*, *6*(4), 363–380.
- Böning, C., and J. Kröger (2005), Seasonal variability of deep currents in the equatorial Atlantic: A model study, *Deep Sea Res. Part I*, *52*, 99–121.
- Boyer, T., and S. Levitus (1997), Objective analyses of temperature and salinity for the world ocean on a 1/4 degree grid, technical report, NOAA, Washington, D. C.
- Brandt, P., and C. Eden (2005), Annual cycle and interannual variability of the mid-depth tropical Atlantic Ocean, *Deep Sea Res. Part I*, *52*, 199–219.
- Brauch, J., and R. Gerdes (2005), Response of the northern North Atlantic and Arctic oceans to a sudden change of the North Atlantic Oscillation, *J. Geophys. Res.*, *110*, C11018, doi:10.1029/2004JC002436.
- Cenedese, C., C. Adduce, and D. Fratantoni (2005), Laboratory experiments on mesoscale vortices interacting with two islands, *J. Geophys. Res.*, *110*, C09023, doi:10.1029/2004JC002734.
- Cherubin, L., and P. Richardson (2007), Caribbean current variability and the influence of the Amazon and Orinoco freshwater plumes, *Deep Sea Res. Part I*, *54*, 1451–1473, doi:10.1016/j.dsr.2007.04.021.
- da Silva, A. M., C. C. Young-Molling, and S. Levitus (Eds.) (1994), *Atlas of Surface Marine Data 1994*, NOAA Silver Spring, Md.
- Dengg, J., C. Böning, U. Ernst, R. Redler, and A. Beckmann (1999), Effects of an improved model representation of overflow water on the subpolar North Atlantic, *Int. WOCE Newsl.*, *37*, 10–15.
- Eden, C., and C. Böning (2002), Sources of eddy kinetic energy in the Labrador Sea, *J. Phys. Oceanogr.*, *32*, 3346–3363.
- Ffield, A. (2005), North Brazil Current Rings viewed by TRMM Microwave Imager SST and the influence of the Amazon Plume, *Deep Sea Res. Part I*, *52*, 137–160.
- Fratantoni, D., and D. Glickson (2002), North Brazil Current ring generation and evolution observed with SeaWiFS, *J. Phys. Oceanogr.*, *32*, 1058–1074.
- Fratantoni, D., and P. Richardson (2006), The evolution and demise of North Brazil Current rings, *J. Phys. Oceanogr.*, *36*, 1241–1264.
- Garraffo, Z., W. Johns, E. Chassignet, and G. Goni (2003), North Brazil Current rings and transport of southern waters in a high-resolution numerical simulation of the North Atlantic, in *Interhemispheric Water Exchange in the Atlantic Ocean*, edited by G. Goni and P. Malanotte-Rizzoli, chap. 15, pp. 375–410, Elsevier Oceanogr. Ser.
- Garzoli, S., A. Ffield, and Q. Yao (2003), North Brazil Current rings and the variability in the latitude of retroflexion, in *Interhemispheric Water Exchange in the Atlantic Ocean*, Elsevier Oceanogr. Ser., vol. 68, edited by G. Goni and P. Malanotte-Rizzoli, chap. 14, pp. 357–374, Elsevier, Amsterdam.
- Garzoli, S., A. Ffield, W. Johns, and Q. Yao (2004), North Brazil Current retroflexion and transports, *J. Geophys. Res.*, *109*, C01013, doi:10.1029/2003JC001775.

- Goni, G., and W. Johns (2003), Synoptic study of warm rings in the North Brazil Current retroflection region using satellite altimetry, in *Interhemispheric Water Exchange in the Atlantic Ocean*, Elsevier Oceanogr. Ser., vol. 68, edited by G. Goni and P. Malanotte-Rizzoli, chap. 13, pp. 335–356, Elsevier, Amsterdam.
- Halliwel, G., Jr., R. Weisberg, and D. Mayer (2003), A synthetic float analysis of upper-limb meridional overturning circulation interior ocean pathways in the tropical/subtropical Atlantic, in *Interhemispheric Water Exchange in the Atlantic Ocean*, Elsevier Oceanogr. Ser., vol. 68, edited by G. Goni and P. Malanotte-Rizzoli, chap. 11, pp. 287–312, Elsevier, Amsterdam.
- Hüttl, S., and C. Böning (2006), Mechanisms of decadal variability in the shallow subtropical-tropical circulation of the Atlantic Ocean: A model study, *J. Geophys. Res.*, 111, C07011, doi:10.1029/2005JC003414.
- Hüttl-Kabus, S., and C. Böning (2008), Pathways and variability of the off-equatorial undercurrents in the Atlantic Ocean, *J. Geophys. Res.*, 113, C10018, doi:10.1029/2007JC004700.
- Jochum, M., and P. Malanotte-Rizzoli (2003), On the generation of North Brazil Current rings, *J. Mar. Res.*, 61, 147–173.
- Johns, W., T. Lee, F. Schott, R. Zantopp, and R. Evans (1990), The North Brazil Current retroflection: Seasonal structure and eddy variability, *J. Geophys. Res.*, 95, 22,103–22,120, doi:10.1029/JC095iC12p22103.
- Johns, W., R. Zantopp, and G. Goni (2003), Cross-gyre transport by North Brazil Current rings, in *Interhemispheric Water Exchange in the Atlantic Ocean*, Elsevier Oceanogr. Ser., vol. 68, edited by G. Goni and P. Malanotte-Rizzoli, chap. 16, pp. 411–441, Elsevier, Amsterdam.
- Kalnay, E., et al. (1996), The NCEP/NCAR 40 year reanalysis project, *Bull. Am. Meteorol. Soc.*, 77(3), 437–471.
- Kirchner, K., M. Rhein, C. Mertens, C. Böning, and S. Hüttl (2008), Observed and modeled meridional overturning circulation related flow into the Caribbean, *J. Geophys. Res.*, 113, C03028, doi:10.1029/2007JC004320.
- Kirchner, K., M. Rhein, S. Hüttl-Kabus, and C. Böning (2009), On the spreading of South Atlantic Water into the Northern Hemisphere, *J. Geophys. Res.*, 114, C05019, doi:10.1029/2008JC005165.
- Kraus, E., and J. Turner (1967), A one-dimensional model of the seasonal thermocline: I. A laboratory experiment and its interpretation, *Tellus*, 19, 88–97.
- Levitus, S., and T. P. Boyer (Eds.) (1994), *World Ocean Atlas 1994*, vol. 4, *Temperature*, NOAA Atlas NESDIS, vol. 4, 129 pp., NOAA, Silver Spring, Md.
- Mertens, C., M. Rhein, M. Walter, and K. Kirchner (2009), Modulation of the inflow into the Caribbean Sea by North Brazil Current rings, *Deep Sea Res. Part I*, 56, doi:10.1016/j.dsr.2009.03.0028.
- Pacanowski, R. (1995), MOM2 documentation, user's guide and reference manual, technical report, 329 pp., Geophys. Fluid Dyn. Lab., Princeton, N. J.
- Rhein, M., K. Kirchner, C. Mertens, R. Steinfeldt, M. Walter, and U. Fleischmann-Wischnath (2005), Transport of South Atlantic water through the passages south of Guadeloupe and across 16°N, 2000–2004, *Deep Sea Res. Part I*, 52, 2234–2249.
- Richardson, P. (2005), Caribbean Current and eddies as observed by surface drifters, *Deep Sea Res. Part II*, 52, 429–463.
- Simmons, F., and D. Nof (2002), The squeezing of eddies through gaps, *J. Phys. Oceanogr.*, 32, 314–335.
- Stramma, L., and F. Schott (1999), The mean flow field of the tropical Atlantic Ocean, *Deep Sea Res. Part II*, 46, 279–303.
- Stramma, L., M. Rhein, P. Brandt, M. Dengler, C. Böning, and M. Walter (2005), Upper ocean circulation in the western tropical Atlantic in boreal fall 2000, *Deep Sea Res. Part I*, 52, 221–240.
- Wilson, W., W. Johns, and S. Garzoli (2002), Velocity structure of North Brazil Current rings, *Geophys. Res. Lett.*, 29(8), 1273, doi:10.1029/2001GL013869.
- Zharkov, V., and D. Nof (2009), Why does the North Brazil Current regularly shed rings but the Brazil Current does not?, *J. Phys. Oceanogr.*, 40, 354–367, doi:10.1175/2009JPO4246.1.

C. W. Böning, Leibniz Institut für Meereswissenschaften, Universität Kiel, Wischhofstr. 1-3, D-24148 Kiel, Germany.

S. Hüttl-Kabus, Bundesamt für Seeschifffahrt und Hydrographie, Bernhard-Nocht-Str. 78, D-20359 Hamburg, Germany.

K. Jochumsen, Institut für Meereskunde, Universität Hamburg, Bundesstr. 53, D-20146 Hamburg, Germany. (kerstin.jochumsen@zmaw.de)

M. Rhein, Institut für Umweltphysik, Abteilung Ozeanographie, Universität Bremen, Otto-Hahn-Allee 1, D-28359 Bremen, Germany.